Measurements of atomic carbon density in processing plasmas by vacuum ultraviolet laser absorption spectroscopy

Norifusa Tanaka[a)] and Kunihide Tachibana[b)]
Department of Electronic Science and Engineering, Kyoto University, Yoshida-Honmachi, Sakyo-ku, Kyoto 606-8501, Japan

Measurements of the absolute C atom density in an inductively coupled plasma (ICP) source were carried out by using vacuum ultraviolet (VUV) laser absorption spectroscopy with the resonance lines of C atoms at wavelengths around 94.5 and 165.7 nm. A tunable VUV laser covering these wavelength ranges was generated by a two-photon resonance/four-wave mixing technique in Xe gas. No absorption at around 94.5 nm could be observed, but from the absorption spectra around 165.7 nm we successfully derived the absolute density of C atoms in the ICP source. The obtained values varied from 1×10^{10} to 1×10^{11} cm^{-3}, depending on the source gas and operating conditions of the plasma source. The relatively small density values compared to other atomic species are attributed to the large loss rates, which mostly occur on the surface. © *2002 American Institute of Physics.* [DOI: 10.1063/1.1513877]

I. INTRODUCTION

There has been much discussion on the roles of C atoms produced in plasmas of fluorocarbon and hydrocarbon gases for various kinds of plasma material processing. For example, in plasma etching processes for the production of ultralarge-scale integration (ULSI) devices, fluorocarbon plasmas have been used for selective etching of SiO_2 on Si, Si_3N_4, and under photoresist. However, the poor reproducibility of the etch rate and inadequate selectivity have sometimes caused severe problems. A sophisticated balance between etching and deposition can achieve the selectivity where not only CF_x $(x = 1 - 3)$ radicals and F atoms but also C atoms may play important roles in the mechanism.[1] In plasma-enhanced chemical vapor deposition (PECVD) processes for diamond and diamond-like carbon films, controversial reports have stated that C atoms in the gas phase have a positive or negative correlation with the characteristics of high mechanical hardness, thermal conductivity, and chemical stability.[2–4]

Recently, in using low-pressure and high-density plasma sources,[5] such as inductively coupled plasma (ICP), electron cyclotron resonance (ECR) plasma, and helicon-wave excited plasma (HWP), the increased dissociation of source gases has made the gas chemistry more complex. Therefore quantitative *in situ* diagnostics of radical densities as well as plasma parameters are necessary to clarify the kinetics of these plasmas in the gas phase and on the surface in order to control those processes more precisely. Although much work has been done on the quantitative measurements of molecular radicals such as CF_x $(x = 1 - 3)$,[6] quantitative and reliable measurements of C and F atoms have not yet been performed. Some methods have been developed for the mea-

surement of these atomic species, such as two-photon absorption laser-induced fluorescence[7,8] and line absorption spectroscopy in the vacuum-ultraviolet wavelength region with conventional (incoherent) light sources.[9,10] However, the former method requires a laser source with a sufficient power level, and absolute density calibration is not an easy task.[11] In the latter method, other errors in the derivation of absolute density have been caused by the influence of background absorption by source gas molecules and species produced in plasma as well as by inaccurate estimation of the line shape of the light source. Therefore we have been developing an absolute measurement system for these species by using vacuum ultraviolet laser absorption spectroscopy (VUVLAS).[12–14] In this method, the VUV laser is generated by a two-photon resonance four-wave mixing technique, and its tunability permits accurate determination of absolute values from the integrated absorption line shapes. This technique has been successfully applied to the measurement of F atoms in the plasmas of various fluorocarbon source gases.[12,13] In this study, we report on measurements of C atom density by the same technique in the wavelength ranges around 94.5 and 165.7 nm. These measurements were performed in an ICP source with various carbon-containing source gases.

II. EXPERIMENTAL PROCEDURE

Figure 1 shows a schematic diagram of the experimental setup for the measurement of C atom density using VUVLAS. In order to generate a tunable VUV laser of wavelengths around 94.5 and 165.7 nm, we used a two-photon resonance/four-wave mixing technique[15,16] in Xe gas ($\nu_{VUV} = 2\nu_1 \pm \nu_2$), as in the case of our previous F atom measurement.[12,13] Two dye lasers pumped simultaneously by a Xe–Cl excimer laser provided the frequencies (wavelengths) of $\nu_1 (= c/\lambda_1)$ and $\nu_2 (= c/\lambda_2)$, where c is the light velocity. The energy of two photons $2h\nu_1$, where h is the

---
[a)]Present address: Mobile Entertainment Co., Pioneer Corp., Yamada, Kawagoe, Saitama 350-8555, Japan.
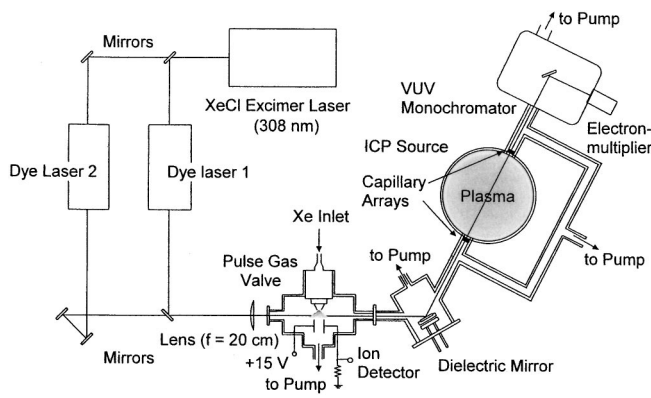[b)]Author to whom correspondence should be addressed; electronic mail: tatibana@kuee.kyoto-u.ac.jp

FIG. 1. Experimental setup for VUVLAS measurement combined with an ICP plasma reactor.

Planck constant, was set in resonance with the energy level of Xe ($2p_1$: Paschen notation) from the ground state at $\lambda_1 = 249.63$ nm (Fig. 2), while λ_2 was varied between 380 and 400 nm or between 504 and 506 nm to obtain a tunable VUV laser in the range from 94.0 to 95.0 nm (in sum-frequency generation scheme) or from 165.6 to 165.8 nm (in difference-frequency generation scheme). The two-photon resonance was adjusted by optimizing the current from (2 +1) photoionization of Xe atoms. Two dye laser beams were aligned collinearly and focused by a lens of $f = 20$ cm into the VUV generation chamber, where these frequencies were mixed to generate ν_{VUV}. In the case of sum-frequency generation, Xe gas was injected into the chamber synchronously with the two lasers, since differential pumping was necessary due to the lack of window materials at this wavelength. On the other hand, in the case of difference-frequency generation, Xe gas was filled in the chamber at a fixed pressure of 20 Torr with a MgF$_2$ sealing window at the exit side. The generated VUV radiation was reflected by the surface of an uncoated concave quartz plate of 1 m curvature, which was placed in another small chamber at an incident angle of 65°. The quartz plate acts partially in collimating the VUV beam and also in separating it from the

fundamental wavelengths, since the reflectivity in the VUV range (expected to be more than 20%) is larger than that for the UV-to-visible range.[17] The VUV laser power was high enough to obtain a reasonable signal-to-noise ratio but low enough to avoid the pumping effect of the lower level of the transition, as checked by changing the power level by a factor of 5.[14]

The ICP chamber was 32 cm in inner diameter and 15 cm in height. A substrate holder of 22 cm in diameter was located 8.5 cm below the quartz plate, and rf (13.56 MHz) power up to 600 W was supplied by a flat spiral four-turn antenna coil into the plasma reactor through a quartz plate of 19 cm in diameter and 1.5 cm in thickness. Source gases (CH$_4$, CF$_4$, CHF$_3$, C$_4$F$_8$, C$_5$F$_8$, and CO) and dilution gas Ar were introduced into the chamber from a side port at a pressure range from 1.3 to 13.3 Pa. The laser beam was fed into the chamber through the capillary array windows mounted on both sides of the chamber at 2 cm above the substrate holder. The VUV laser path was differentially pumped, so the windows also functioned to sustain the pressure difference. In this configuration, the absorption length was close to the inner diameter of the chamber and was taken to be 32 cm. The VUV probe beam coming out of the chamber was further filtered by a VUV monochromator of $f = 20$ cm and detected by a Cu–BeO electron multiplier for the 94.5 nm range and by a solar blind photomultiplier for the 165.7 nm range.

The partial energy level diagram of C is shown in Fig. 2 together with that of the Xe atom to illustrate the relatioship between the generated VUV laser and the absorption measurement. The measurement was performed on the $2s^2 2p^2\,^3P_J - 2s2p^3\,^3S_1^o\ (J=0, 1, 2)$ transition at around 94.5 nm and the $2s^2 2p^2\,^3P_J - 2s^2 2p3s\,^3P_J^o\ (J=0, 1, 2)$ transition at around 165.7 nm. Provided that the corresponding transition probability A_{ul} is known, the absolute density populated on each lower level N_l can be derived from the integrated area of the profile of absorption coefficient per unit length $k_{ul}(\nu)$ as

$$N_l = \frac{8\pi g_l}{\lambda_0^2 g_u A_{ul}} \int k_{ul}(\nu) d\nu, \tag{1}$$

where λ_0 is the wavelength and g_l and g_u are the statistical weights of the lower and upper levels of the transition. It is noted here that an obtained value of N_l gives inherently the averaged value over the line-of-sight (the absorption length was assumed to be 32 cm as stated above).

The effect of background absorption due to source gas and product species can be eliminated by scanning the laser frequency as explained previously.[12] The estimated error in the determination of N_l mainly comes from the data reproducibility (10%–20%), uncertainty in the evaluation of the $k_{ul}(\nu)$ profile for the integration (~20%), and the uncertainty in the reported value of the transition probability (10%). Therefore the total error may amount up to 30%.

III. EXPERIMENTAL RESULTS

First, we attempted a VUVLAS measurement at the $2s^2 2p^2\,^3P_J - 2s2p^3\,^3S_1^o\ (J=0, 1, 2)$ transition around 94.5
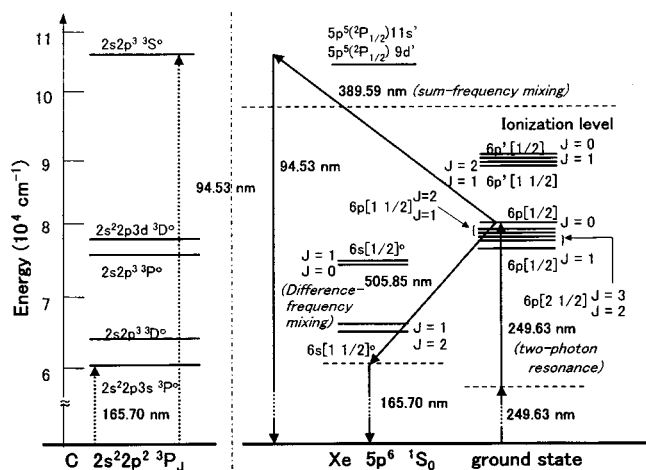

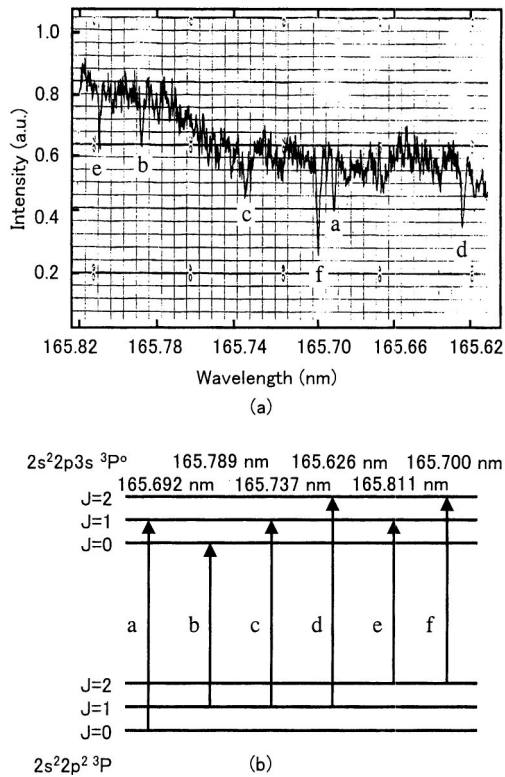FIG. 2. Partial energy level diagrams of Xe and C atoms as explanations of VUV generation and VUVLAS measurement.

FIG. 3. (a) Measured absorption spectra and (b) corresponding transitions of resonance lines within the $2s^22p^2\,^3P_J-2s^22p3s\,^3P_J^{\,o}$ ($J=0$, 1, 2) group.

FIG. 4. Typical absorption line profile of 165.700 nm ($2s^22p^2\,^3P_2-2s^22p3s\,^3P_2^{\,o}$) line.

nm, since the literature values of the transition probability are extremely large: 3.79×10^8, 1.14×10^9, and $1.89\times10^9\,\mathrm{s}^{-1}$ for the 94.52, 94.53, and 94.56 nm lines, respectively,[18] and the wavelengths are close to those of F atoms which we have measured previously.[12,13] However, no absorption signal could be observed within the scanned wavelength range from 94.0 to 95.0 nm, although various source gases including CO and fluorocarbon gases were tested. Then, we tried to observe the emission at around 94.5 nm in the ICP source operated with pure source gases and also in a dc discharge in Ar with a carbon hollow cathode operated at a pressure of 4.0 Pa and a current of 20 mA. Unfortunately, we were not able to observe any emission spectra at around 94.5 nm in either case, although in the latter case closely lying Ar$^+$ lines might have obscured the emission.

Then, we proceeded to the VUVLAS measurement at the 165 nm ($2s^22p^2\,^3P_J-2s^22p3s\,^3P_J^{\,o}$) transition group. The signals observed in the spectral range between 165.62 and
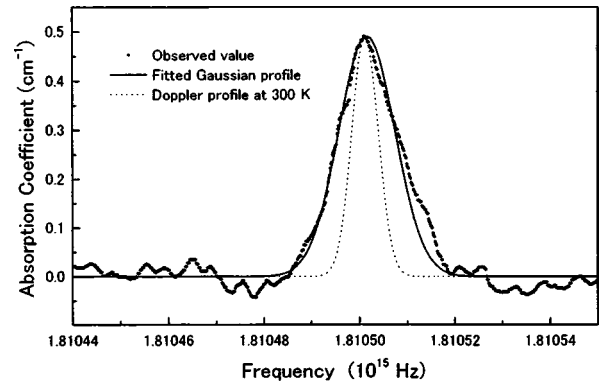
165.82 nm in CO/Ar plasma are shown in Fig. 3(a). The flow rates of CO and Ar gases were 10 and 20 sccm (standard cm^3/min), the total pressure was 4.0 Pa, and the supplied rf power was 400 W. The absorption feature composed of the six isolated lines in Fig. 3(b) is clearly seen in this result owing to the fairly high resolution of our VUVLAS technique. The C atom densities derived from these six absorption lines using Eq. (1) are listed in Table I. Assuming the Boltzmann distribution within the ground state levels at a temperature of 300 K, the ratio of C atom densities on the $^3P_2$, $^3P_1$, and $^3P_0$ levels divided by the respective statistical weights should be 0.809:0.926:1. From Table I, it is evident that C atom densities obtained from these absorption lines nearly correspond to this ratio except for the value from the 165.700 nm line. If we suppose that overestimation of the transition probability is the cause of this disagreement, the transition probability of 165.700 nm predicted from this result would be smaller than the reported value[18] by about 20%. In order to ascertain the transition probability ratios, we tried to measure the intensity ratios of emission lines within the 165 nm group from the same carbon hollow cathode discharge used above. In this case, emission peaks around 165.7 nm were observed, but the six lines could not be fully resolved due to the limited resolution of the VUV monochromator used.

Figure 4 shows an example of the absorption coefficient $k_{ul}(\nu)$ as a function of frequency ν for the 165.700 nm ($2s^22p^2\,^3P_2-2s^22p3s\,^3P_2^{\,o}$) line. Its full width at half maximum (FWHM) was estimated to be 1.43×10^{-3} nm, which was about two times larger than that of the Doppler profile at 300 K, i.e., 0.685×10^{-3} nm. The difference may

TABLE I. Population densities on ground state levels ($l\equiv J=0$, 1, 2) measured with various absorption lines.

Lower energy level	Statistical weight g_l	Wavelength (nm)	Transition probability ($10^8\,\mathrm{s}^{-1}$)	Measured density N_l (cm^{-3})	Normalized density N_l/g_lN_0	Normalized Boltzmann factor
$2s^22p^2\,^3P_0$	1	165.692	1.13	1.65×10^{10}	1	1
$2s^22p^2\,^3P_1$	3	165.789	3.43	3.98×10^{10}	0.804	0.926
$2s^22p^2\,^3P_1$	3	165.737	0.864	4.19×10^{10}	0.846	0.926
$2s^22p^2\,^3P_1$	3	165.626	0.858	3.97×10^{10}	0.802	0.926
$2s^22p^2\,^3P_2$	5	165.811	1.44	6.56×10^{10}	0.795	0.809
$2s^22p^2\,^3P_2$	5	165.700	2.52	4.17×10^{10}	0.505	0.809

J. Appl. Phys., Vol. 92, No. 10, 15 November 2002

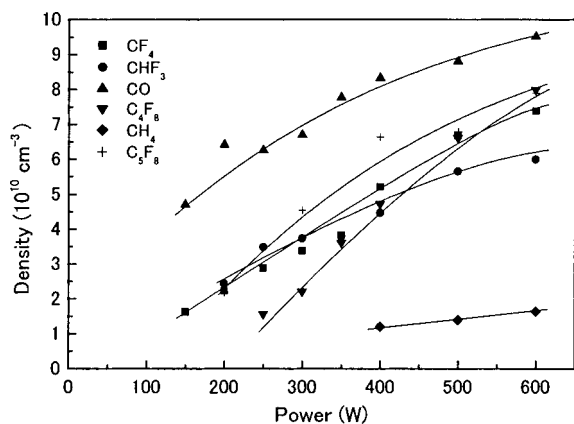N. Tanaka and K. Tachibana   5687

FIG. 5. rf power dependence of C atom densities measured in plasmas of fluorocarbon, methane, and CO gases at a total pressure of 2.7 Pa with flow rates of source gas and Ar of 10 and 20 sccm, respectively.
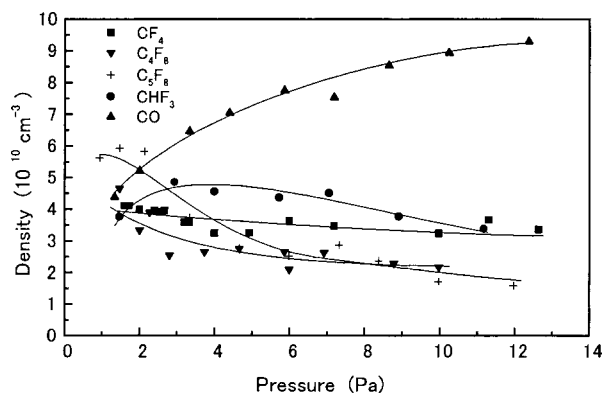

FIG. 6. Pressure dependence of C atom densities measured in plasmas of fluorocarbon, methane, and CO gases at rf power of 300 W with flow rates of source gas and Ar of 10 and 20 sccm, respectively.

be attributed mostly to the finite spectral width of our VUV laser, but another contributing factor may be the nonthermalized velocity distribution of C atoms produced by electron collisional dissociation. Nevertheless, the absolute density can be derived accurately from the integrated area of $k_{ul}(\nu)$ over the absorption coefficient profile given in Eq. (1) without any influence of the instrumental width. We used this 165.700 nm line representatively for the rest of the measurements because its absorption was the largest among the six lines. The total density of three levels, $N = \Sigma_l N_l$, in the ground state was estimated by using the experimental ratio given in Table I.

The absolute C atom density in the ground state measured in various source gases as a function of rf power is shown in Fig. 5. Each source gas with a flow rate of 10 sccm was admixed with Ar gas with 20 sccm, and the total pressure was kept at 2.7 Pa. Measured values of N were on the order of 10^{10} cm^{-3}, and in all gases density increased monotonically with rf power. The measured C atom density in fluorocarbon plasmas was much smaller than the F atom density, which had been measured previously as being on the order of 10^{12} cm^{-3}.[12,13] The C atom density in CO plasma is larger than the values measured in fluorocarbon plasmas, while a saturating tendency is seen as rf power increases. On the other hand, the values of N in CH$_4$ plasma are much smaller than those in fluorocarbon plasmas, and it drops below the detection limit at an rf power under 400 W.

Figure 6 shows the C atom density measured in various source gases as a function of total pressure. The supplied rf power was kept at 300 W, and the flow rates of source gas and Ar were 10 and 20 sccm, respectively. The values of N in CO plasma increased with pressure almost to 1×10^{11} cm^{-3}, although a saturating tendency could be seen as in the case of power dependence. On the other hand, in fluorocarbon plasmas, the density decreased gradually with pressure from $(3-5) \times 10^{10}$ to $(1-3) \times 10^{10}$ cm^{-3}.

IV. DISCUSSION

We first discuss the reason why the absorption signals of the 94.5 nm transition group were not detected in spite of the very large transition probability values previously reported.[18]

Assuming the C atom density measured from the 165 nm transition group, the expected absorption at 94.5 nm lines should be 50%. If this were the case, the absorption signal could be found without any difficulty unless the tuning range of our experiment was completely misaligned, which is of little possibility. In order to check the validity of the transition probabilities, we tried to detect those lines with optical emission. However, we could not succeed in this detection. Consequently, we suspect that the reported values of the transition probability might be overestimated by more than an order of magnitude. There remains, however, a slight possibility that the intensity of those emission lines could be very small if the population on the corresponding upper level $(2s2p^3 \, ^3S_1^o)$ was very small in our plasma.

Next, we discuss the large differences between the present values of C atom density and those reported previously by Ito et al.[19,20] They measured it by using an ultraviolet absorption spectroscopy (UVLAS) technique with a carbon hollow cathode lamp as the light source. The transition used was $2s^2 2p^2 \, ^3P_2 - 2s2p^3 \, ^5S_2$ at 296.7 nm, which is a forbidden line, and the obtained values were on the order of 10^{14} cm^{-3}. They also determined the transition probability to be 3.9×10^4 s^{-1} from the decay rate of the emission line.[20] However, another theoretical value of 5.3×10^8 s^{-1} was reported for the transition probability of the line,[21] which is about 10^4 times larger than their estimated value. If the C atom density were derived from this transition probability, it would be on the order of 10^{10} cm^{-3}, which is consistent with the present measurement.

The major mechanism for the production of C atoms in a plasma is the electron collisional dissociation of parent gases or radicals; another possible process results from the sputtering of polymer films deposited on the chamber wall. Suzuki et al. suggested that C and C$_2$ radicals are produced mostly by ion-enhanced chemical reactions with fluorocarbon films on the chamber wall.[22] In order to estimate the contribution of the sputtering effect in our experiment, the C atom density in pure Ar plasma was measured after seasoning by CF$_4$/Ar plasma. As shown in Fig. 7, the C atom density in Ar plasma was about half of that in CF$_4$/Ar plasma. This result indi-
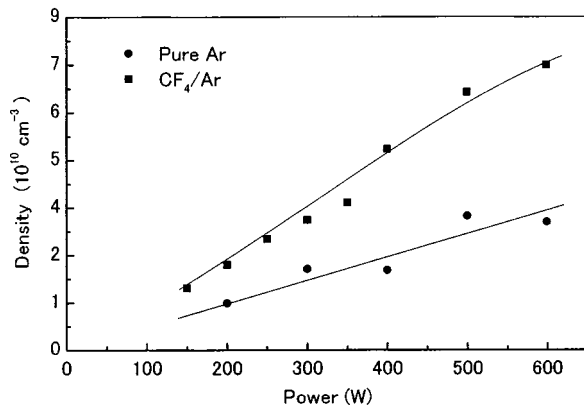
FIG. 7. C atom densities measured in CF_4/Ar plasma and in pure Ar plasma after seasoning with CF_4/Ar plasma as a function of rf power.

cates that C atoms were generated not only by dissociation reactions in the gas phase but also by sputtering the polymer films on the wall surface. However, the former contribution was shown to be larger in most of the tested gases under our experimental conditions.

Here, we consider the reason why the present values of C atom density are much smaller than the reported values of other atomic species such as H, F, and O under similar conditions. For example, in CO plasma the following electronic processes are possible for the production of C atoms in the gas phase by the electron collisional dissociation:

$$CO + e^- \rightarrow C + O + e^-, \tag{2}$$

$$CO + e^- \rightarrow C + O^-. \tag{3}$$

The estimated rate constant for the dissociative attachment process [reaction (3)] is $k = 10^{-14} - 10^{-13} \, cm^3 \, s^{-1}$, which is much smaller than the rate constant for the direct dissociation process [reaction (2)] of $k = (0.03 - 3) \times 10^{-11} \, cm^3 \, s^{-1}$.[23,24] Thus it can be said that in CO plasma C atoms are produced predominantly by the direct process. In general, the C atom density N at a steady state is determined by the balance between the production and loss rates as

$$dN/dt = k_p n_e N_{CO} - R_l N = 0, \tag{4}$$

where n_e is the electron density, N_{CO} is the density of parent CO molecules, k_p is the production rate constant, and R_l is the total loss rate. If we take the above value of k for reaction (2) as k_p and assume typical values of n_e as $10^{10} - 10^{11} \, cm^{-3}$ and N_{CO} as $3 \times 10^{14} \, cm^{-3}$, R_l should be about $10^3 - 10^5 \, s^{-1}$ to be consistent with the measured N values of $10^{10} - 10^{11} \, cm^{-3}$. The loss mechanisms are reactions in the gas phase and on the wall surface. Possible reactions of C atoms in the gas phase are the recombination processes:

$$C + O \rightarrow CO, \tag{5}$$

$$C + C \rightarrow C_2, \tag{6}$$

$$C + CO \rightarrow C_2O. \tag{7}$$
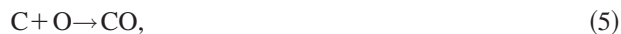
All of these are three-body reactions whose rate constants are reported as 3×10^{-33}, 2×10^{-34}, and $6.3 \times 10^{-32} \, cm^6 \, s^{-1}$, respectively.[9,25] Under our low-pressure condition, the rates

of these reactions become less than $10^{-1} \, s^{-1}$, even if the total gas density is taken as the third-body density, and thus such reactions cannot explain the main loss process. There is also a two-body rate constant for reaction (6) as $2.2 \times 10^{-11} \, cm^3 \, s^{-1}$.[26] Even with this value, the rate of this reaction is only $2.2 \times (10^{-1} - 10^0) \, s^{-1}$.

Accordingly, we have to attribute the major loss mechanisms to the surface reactions. In order to substitute the surface loss rate with the equivalent volume loss rate R_l, let us assume that the total flux of C atoms is equal to the loss rate in the entire volume as $\Gamma S = R_l V N$, where Γ is the flux per unit surface, S is the total surface area, and V is the volume. If we assume that Γ is determined by the free flux as $\Gamma = (\bar{v}/4)N$, where $\bar{v}$ is the thermal velocity of C atoms at 300 K, R_l is estimated to be on the order of $10^4 \, s^{-1}$. Otherwise, if we take the diffusion flux given by $\Gamma = (D_0/p\Lambda^2) \times (V/S)N$, where D_0 is the diffusion coefficient at 1 Torr, Λ is the characteristic diffusion length given by $1/\Lambda^2 = (\pi/L)^2 + (2.4/R)^2$ with the height L and radius R of the chamber, and p is the total pressure, the result for R_l stays on the same order with a typical value for D_0 of $3 \times 10^4 \, cm^2 \, Pa$.[10] This is consistent with the required loss rate derived above. In this evaluation, it is assumed that the flux of C atoms is completely lost at the wall. In the cases of other atomic species, the wall loss probabilities are expected to be very small. As the mechanism of wall loss, the association process [reaction (6)] or further agglomeration reactions such as

$$C + C_x \rightarrow C_{x+1} (x \geq 2) \tag{8}$$

could be plausible processes that utilize the wall surface as a third body.

In fluorocarbon plasmas, the obtained C atom density increases almost linearly with input power except for the case of CHF_3 plasma. In these kinds of plasmas, the electron collisional dissociation of parent gases are expected to be followed by the successive dissociation of radicals, e.g., from CF_2 and CF radicals to C atoms;

$$CF_2 + e^- \rightarrow CF + F + e^- \text{ or } C + 2F + e^-, \tag{9}$$

$$CF + e^- \rightarrow C + F + e^-. \tag{10}$$
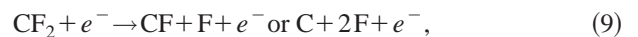
Miyata et al. reported that the density of CF_2 radicals measured in an ECR plasma using infrared laser absorption spectroscopy (IRLAS) is on the order of $10^{12} - 10^{13} \, cm^{-3}$, while the density of CF radicals is on the order of $10^{10} - 10^{11} \, cm^{-3}$.[6] These results are consistent with our data obtained in a parallel plate reactor.[27] If we suppose that the second channel of reaction (9) is the major source for the production of C atoms and that the rate constant is the same as that of the first channel: $k = 3.3 \times 10^{-10} \, cm^3 \, s^{-1}$,[28] the estimated production rate would be able to reach the same order as in the case of CO plasma. However, the probability of the second channel might not be so large due to the larger threshold energy. If the production were mainly from CF radicals through reaction (10), the production rate would be much lower. The observed density of C atoms in fluorocarbon plasmas is actually smaller than that in CO plasma, but it does not differ by more than one order of magnitude. This

suggests that the loss rate R_l in fluorocarbon plasmas may be smaller when the wall surface is covered with a polymer film instead of a carbon-aggregated material without a fluorine component.

In CHF$_3$ plasma, a saturating tendency was observed in the higher power region. The recombination reactions with H and H$_2$, that is,

$$C+H\rightarrow CH, \tag{11}$$

$$C+H_2\rightarrow CH+H, \tag{12}$$

might be conceivable loss processes since H and H$_2$ are produced more abundantly as rf power increases. However, the former is a three-body reaction and the latter is an endothermic reaction with an enthalpy change of $\Delta H = 97.1$ kJ/mol;[3] consequently, these reactions can only have a minor influence on the loss process of C atoms. Binary reactions with CH$_2$ and CH$_3$ might be alternative processes, as in the case of CH$_4$ plasma mentioned below.

It is surprising that the values in CH$_4$ plasma are smaller than those in fluorocarbon plasmas, although the C–H bond energy of 3.5 eV is smaller than the C–F bond energy of 5.6 eV. It is likely in CH$_4$ plasma that C atoms are generated in stepwise processes via CH$_3$, CH$_2$, and CH. If we suppose that CH radicals are the main source, the density would determine the production rate of C atoms, whose values may be around 10^{10} to 10^{11} cm^{-3}, as estimated from the values obtained previously in a parallel plate reactor.[29] The relatively small density of CH is possibly due to the large loss rate by the reaction

$$CH+CH_4\rightarrow C_2H_5, \tag{13}$$

which has a reported rate constant of $k=1.0\times10^{-10}$ cm^3 s^{-1}.[9]

Regardless of the reason for small CH density, the production rate of C atoms becomes smaller than that in the CO plasma by one to two orders of magnitude, even when the rate constant is assumed to be ten times larger than k assigned for reaction (2) and n_e is the same. In addition, the loss rate may be large due to the following reactions:

$$C+CH_2\rightarrow C_2H+H, \tag{14}$$

$$C+CH_3\rightarrow C_2H+H_2 \text{ or } C_2H_2+H, \tag{15}$$

with a relatively large rate constant of 8.3×10^{-11} cm^{-3} s^{-1} in both cases.[30]

Finally, we discuss the difference in the behavior of C atoms measured in a CO plasma as a function of gas pressure from those in fluorocarbon plasmas shown in Fig. 6. The reason may be attributed to the increase in the loss rate of C atoms with pressure through the three-body reaction with source fluorocarbon molecules. A saturating tendency in the CO plasma may be due to the association reaction between C atoms in the gas phase as pressure increases. A similar behavior was observed previously in the case of F atoms, where the density of F atoms increased monotonically up to 5.3 Pa but started to decrease in the higher pressure region.[13] In addition to those reactions, the change in plasma parameters does influence the production rate of C atoms as pressure changes. For a more quantitative argument, however, we need to have data on the behavior of plasma parameters such as electron density and temperature.

V. CONCLUSIONS

A tunable VUV laser in the 94.5 and 165.7 nm ranges was generated by the two-photon resonance/four wave mixing technique in Xe gas, and the absolute atomic carbon density in an ICP source was successfully measured by using absorption spectroscopy. C atom density increased with an increase in rf power in all of the tested source gases at applied power of 150–600 W. When the pressure was varied, the density behaviors were different between fluorocarbon and CO source gases. The absolute values of C atom density were on the order of 10^{10} cm^{-3}, which are much smaller than the measured values of other atomic species such as F and O under similar conditions.[14] The major reason for this result is attributed to the larger wall loss rate of C atoms, especially when the wall is covered with carbon-aggregated material.

Although the measured density of C atoms is relatively small, this does not necessarily mean that the contributions of C atoms to various processes are negligible. The small density is mainly due to the large loss rate, especially in CO plasma, and the production rate may not be small. Therefore in order to argue the beneficial or deleterious contributions of C atoms in specific material processes, such as the selective etching of SiO$_2$ on Si and under photoresist or the deposition of diamond and diamond-like carbon films, it is necessary to systematically measure C atoms and carbon aggregomers C$_x$ ($x\geqq2$) together with other radicals such as CF$_x$, CH$_x$ ($x=1-3$), and larger polymerized species while giving attention to the etching and deposition characteristics. For this purpose, the present study has shown that the VUVLAS method is a useful tool for the absolute measurement of C atoms.

[1] S. Den, T. Kuno, M. Ito, and M. Hori, J. Vac. Sci. Technol. A **15**, 2880 (1997).

[2] M. E. Coltrin and D. S. Dandy, J. Appl. Phys. **74**, 5803 (1993).

[3] B. W. Yu and S. L. Girshick, J. Appl. Phys. **75**, 3914 (1994).

[4] K. Teii, H. Ito, M. Hori, T. Takeo, and T. Goto, J. Appl. Phys. **87**, 4572 (2000).

[5] M. Lieberman and A. J. Lichtenberg, *Principles of Plasma Discharge and Materials Processing* (Wiley, New York, 1994).

[6] K. Miyata, M. Hori, and T. Goto, J. Vac. Sci. Technol. A **14**, 2343 (1996).

[7] P. Das, G. S. Ondrey, N. van Veen, and R. Bersohn, J. Chem. Phys. **79**, 724 (1983).

[8] G. C. Herring, M. J. Dyer, L. E. Jusinsky, and W. K. Bischel, Opt. Lett. **13**, 360 (1988).

[9] D. Husain and L. J. Kirsch, Trans. Faraday Soc. **67**, 2025 (1971).

[10] H. Ito, K. Teii, H. Funakoshi, M. Ito, and T. Goto, J. Appl. Phys. **88**, 4537 (2000).

[11] A. Goehlich, T. Kawetzki, and H. F. Doebele, J. Chem. Phys. **108**, 9362 (1998).

[12] K. Tachibana and H. Kamisugi, Appl. Phys. Lett. **74**, 2390 (1999).

[13] K. Tachibana, H. Kamisugi, and T. Kawasaki, Jpn. J. Appl. Phys., Part 1 **38**, 4367 (1999).

[14] K. Tachibana, Plasma Sources Sci. Technol. **11**, A166 (2002).

[15] R. Hilbig and R. Wallenstein, IEEE J. Quantum Electron. **QE-19**, 194 (1983).

[16] H. F. Döebele, U. Czarnetzki, and A. Goehlich, Plasma Sources Sci. Technol. **9**, 477 (2000).

[17] R. W. Falcone and J. Bokor, Opt. Lett. **8**, 21 (1983).

[18] W. L. Wiese and G. A. Martin, *Wavelengths and Transition Probabilities for Atoms and Atomic Ions*, NSRDS-NBS 68 (U.S. Government Printing Office, Washington, DC, 1980); see also http:physics.nist.gov/asd. The transition probabilities in the latter reference, which have been used in the present data analyses, are smaller than those in the former reference by 15%–20% for the relevant transitions.

[19] H. Ito, M. Ikeda, M. Ito, M. Hori, and T. Goto, Jpn. J. Appl. Phys., Part 2 **36**, L880 (1997).

[20] H. Ito, M. Ito, M. Hori, A. Kono, and T. Goto, Jpn. J. Appl. Phys., Part 2 **36**, L1616 (1997).

[21] R. Rayling and P. Larkins, *Optical Emission Lines of the Elements* (Wiley, Chichester, 2000).

[22] C. Suzuki, K. Sasaki, and K. Kadota, Jpn. J. Appl. Phys., Part 1 **38**, 6896 (1999).

[23] A. I. Maksimov, L. S. Polak, A. F. Sergienko, and D. I. Slovetskii, High Energy Chem. **13**, 311 (1979).

[24] T. G. Beuthe and J. S. Chang, Jpn. J. Appl. Phys., Part 1 **36**, 4997 (1997).

[25] A. R. Fairbaim, Proc. R. Soc. London, Ser. A **312**, 207 (1969).

[26] F. F. Martinotti, M. J. Welch, and A. P. Wolf, Chem. Commun. (London) **1968**, 115 (1968) through NIST Chemical Kinetics Database No. 17 (1998).

[27] K. Takahashi, A. Itoh, T. Nakamura, and K. Tachibana, Thin Solid Films **374**, 303 (2000).

[28] T. Kimura and K. Ohe, Plasma Sources Sci. Technol. **8**, 553 (1999).

[29] K. Tachibana, T. Mukai, A. Yuuki, Y. Matsui, and H. Harima, Jpn. J. Appl. Phys., Part 1 **29**, 2156 (1990).

[30] J. M. Larson, M. T. Swihart, and S. L. Girshick, Diamond Relat. Mater. **8**, 1863 (1999).